Experimental study of creep of hardened Portland cement paste at variable water content

Z. P. BAŽANT (1), A. A. ASGHARI (2), J. SCHMIDT (3)

Tests of creep under axial load and torque have been made using tubular specimens of extremely small wall thickness (0.7 mm) in order to achieve sufficiently rapid moisture exchange with the environment. The changes of relative humidity and temperature in a program-controlled environmental chamber have been gradual, so as to minimize the differences in pore humidity throughout the specimen wall and the accompanying residual stresses and microcracking. A number of different humidity and temperature histories, including the drying before and during the creep test, and the humidity changes during the creep test and during the recovery, have been tested. The measurements have revealed a decline of the slope of creep curve in log-time after a sufficiently long drying period; acceleration of creep as well as recovery by both drying and wetting; a smaller and more delayed acceleration at lower humidities; a delay of this acceleration with respect to the weight loss; a similarity of these effects in axial and torsional creep; a higher recovery as well as creep at higher humidities when moisture equilibrium has been approached before loading; a higher creep acceleration by temperature increases or decreases when the humidity is below saturation, but a smaller acceleration at nearly dry state; and other effects.

1. INTRODUCTION AND OBJECTIVE OF STUDY

Variations of water content have a major effect on the creep of concrete. This fact has been recognized long ago but, a full, satisfactory knowledge has not been acquired to date, despite extensive experimental and theoretical studies of the moisture effect. Perhaps the most important factor which has been impeding experimental research is the extreme smallness of the rate of moisture migration through uncracked hardened cement paste and concrete. For example, when the standard 6-inch diameter test cylinders are used, their core takes over 10 years to dry to a constant humidity. Consequently, the creep as well as shrinkage in the core is entirely different from that near the surface of the specimen, which produces internal self-equilibrating residual stresses of nonhomogeneous distribution within the specimen, and so the observed creep as well as shrinkage is not directly associated with any simple stress state.

The way to eliminate these difficulties is, of course, to drastically reduce the size of the specimen. The drying time is roughly proportional to the square of the specimen size (even when the nonlinearity of the drying problem is accounted for [5]), and thus, e. g., when a thin-walled specimen of 1 mm wall thickness is used the drying process reaches in one day the same stage as a 6-inch cylinder reaches in about 16 years. One objection against using a specimen so thin is that it cannot be made of concrete, not even of mortar, but only of pure cement paste. Thus, the specimen is not exactly representative of concrete. However, it has been well documented in the literature on creep (e. g. [2]) that the creep responses of cement paste and of concrete are completely similar over the entire service stress range provided that the contribution of microcracking to concrete creep is negligible, and that all of the creep of the concrete originates from the diffusion processes within the cement gel [2].

(1) Professor of Civil Engineering, Northwestern University Evanston, Illinois; Active Member, RILEM.

(2) Graduate Research Assistant, Northwestern University, Evanston, Illinois.

(3) Research Technician, Northwestern University, Evanston, Illinois.

The difference between the creep of concrete and that of cement paste then consists merely of the elastic restraining effect of the aggregate, which reduces the relative magnitude of the creep but does not appreciably alter the time response. In this light, the use of very thin pure cement paste specimens gives information which is also relevant for concrete.

The purpose of this study is to report on an extensive experimental investigation in which the creep of cement paste was measured using novel thin-walled specimens of 0.71 mm wall thickness, whose production technique has been developed previously [3]. The specimens have been much thinner than any other tested before for creep (*cf.* [3]) and have allowed creep measurement at a quasi-equilibrium change of moisture content in the specimen. The main variable which has been studied in the test program is the variation of environmental humidity. As secondary variables, the effect of temperature change, a change in the stress, the recovery of creep, cycling of the load, and the simultaneous action of torque and axial load have been also investigated.

The rate of change of average pore humidity in the specimen is much higher than it is in actual concrete structures. This makes the effects on strain more conspicuous, but suggests caution in quantitative applications to structures.

2. EXPERIMENTAL METHOD

2.1. Thin-walled test specimens

The test specimens were hollow cylindrical tubes of wall thickness 0.71 mm, external diameter 15 mm, and length 92 ± 3 mm. The dimensions guaranteed sufficient margin of safety against local as well as overall instability of the shell. The axial compression strength of the specimen in the wet condition at 22°C (and after 28-day curing at 25°C) was 37.92 N/mm² and the initial tangent Young's modulus was 19.0 kN/mm², the stress-strain diagram being curved and irreversible. After 6 weeks of drying at 50 % relative humidity the compressive strength was 48.05 N/mm², the Young's modulus was 23.8 kN/mm², and the stress-strain diagram was perfectly linear up to failure and perfectly reversible on first unloading and first reloading.

Development of a production technique for the specimens appeared to be a major task. It was successfully accomplished by using a special teflon mold [3] reinforced by aluminium and utilizing to advantage the fact that the thermal contraction on cooling is about 15-times higher for teflon (62×10^{-6} per °C, average between 25°C and 0°C) than it is for cement paste and aluminium. Consequently, the teflon mandrel forming the interior surface of the tube contracts in diameter when cooled in ice water while the teflon forming the exterior surface of the tubular specimen is pulled toward the aluminium case which has a far smaller thermal contraction. This technique allows unmolding of the "egg-thin" shell specimen without cracking in most of the cases. Formation of bubbles and holes in the walls of specimen is prevented by the design of the mold which leads to a high, uniformly distributed pressure in the fresh cement paste mix as the mold is being closed by a bolt. In full detail *see* reference [3].

All specimens were made from Portland Cement 20687, ASTM Type I, using water-cement ratio of 0.45 (by weight). The paste was mixed under vacuum and the specimen was cured in the mold for 1 day at 25°C and 100 % relative humidity. Then each specimen was unmolded and cured until the age of 28 days in a water bath of temperature 25°C, containing lime to prevent carbonation. Subsequently, each specimen was placed in a lime water bath of temperature 2°C and was kept in this bath until the test. Before placement in the loading device the ends of each specimen were ground to achieve perfectly flat end surfaces, normal to the axis of the tube. During this operation and the transfer to the test chamber the specimen's surface was kept moist at all times. Prior to the test, each specimen was weighed under water to check the exact value of the average wall thickness; the average thickness of all specimens tested was 0.713 mm and the standard deviation of the average wall thickness

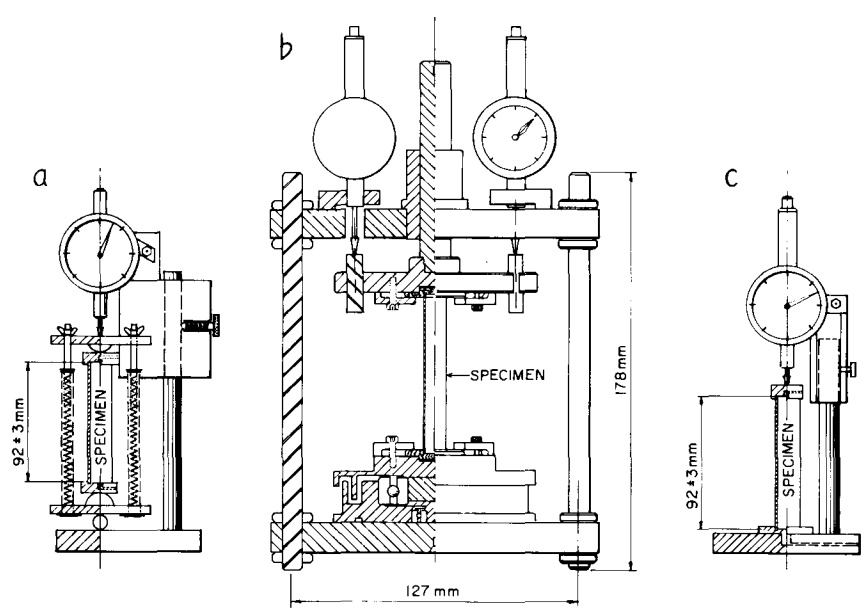

Fig. 1. — Loading and measuring devices : (*a*) for axial creep; (*b*) for axial and torsional creep; (*c*) for shrinkage.

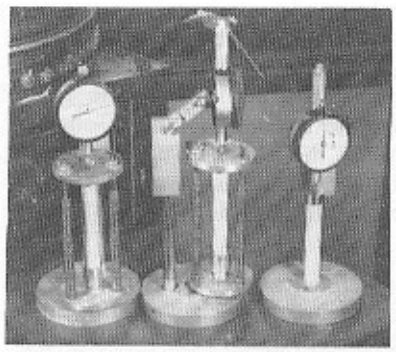

(a)

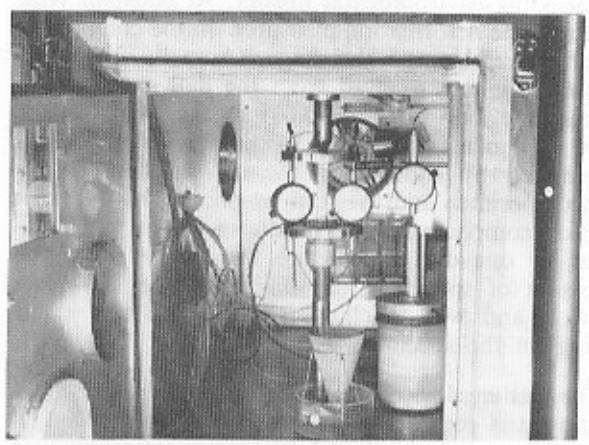

(b)

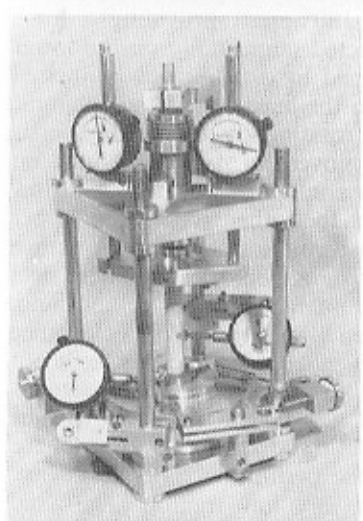

(c)

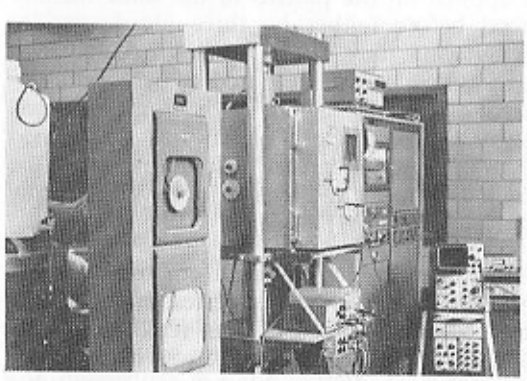

(d)

Fig. 2. — (a) Test devices of axial creep and shrinkage; (b) test arrangement in environmental chamber, loading by machine; (c) device for combined axial and torsional creep; (d) environmental chamber in the MTS frame, and environmental control panel.

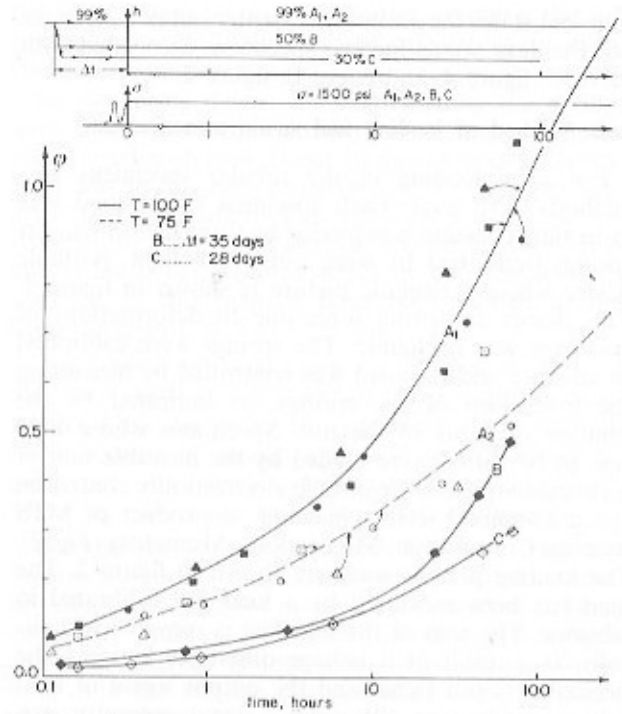

Fig. 3. — Axial creep at various humidities after predrying ($10^6\ \varepsilon_{0.2}$ for $A_1 \ldots 675$, $A_2 \ldots 645$, $B \ldots 623$, $C \ldots 703$; curves A_1 and A_2 are averages from 3 specimens each).

of individual specimens was $\pm$ 0.037 mm. The magnitude of the load was adjusted from specimen to specimen so as to give always the correct stress value. Within the specimens there have been small random variations of local wall thickness over the perimeter as well as over the length of the tube. For testing of the failure behavior (which largely depends on the weakest part of the specimen), the local random variations of wall thickness might prove detrimental, but for observing the deformation behavior they were deemed to be insignificant because the overall deformations (in the service stress range) depend mainly on the average wall thickness but not on its local random deviations. (It would have been possible to control the wall thickness with a greater accuracy, but because of the inherent increase in cost, this was not considered to be worthwhile.)

The purpose of placing each specimen in a refrigerator after 28-days of curing was to allow considerable freedom in choosing the time of starting the test. At the temperature of 2°C the hydration process in the specimen is nearly arrested, and the final degree of hydration is nearly the same (i. e., corresponding to 28-days) independently of the period of storage in the refrigerator. (This is, of course, not true exactly, because cooling reduces the rates of various reactions involved in hydration by different ratios.) The actual period of storage at 2°C varied arbitrarily from 102 days to 490 days, as convenient.

Because of limitations of time, most of the plotted curves in figures are based on a single specimen (with a companion, of course). However, in a number of cases, tests have been repeated two-or three-times to check the scatter and reproducibility of results. Especially consistent were the results for the cases of constant humidity (*see* the comparison of data points for three specimens in figure 3, curves A_1, A_2). In

transient states the scatter was greater but not excessive (see the data points for two specimens associated with curve C, figure 4, and curve E, figure 5.

2.2. Method of loading and strain measurement

For axial loading of the tubular specimens two methods were used. Each specimen whose load was to be time-constant was loaded by three helical tension springs (tensioned by wing nuts) in a light, portable device whose schematic picture is shown in figure 1. The change of spring force due to deformations of specimen was negligible. The springs were calibrated in advance and the load was controlled by measuring the extensions of the springs, as indicated by the number of turns of the nut. Specimens whose load was to be varied were loaded by the movable ram of a closed-loop electrohydraulic electronically controlled (programmable) testing machine, a product of MTS Systems Corporation, Minneapolis, Minnesota (*Fig.* 2). The loading platens used are shown in figure 2. The load has been measured by a load cell calibrated in advance. The ram of the machine is moved hydraulically as a result of a voltage difference between the prescribed input signal and the output signal of load cell or strain gage. "Wavetek" signal generator was used to produce the input signal for cyclic loading, which was always sinusoidal, of frequency 1 Hz.

The axial strain was measured by mechanical dial gages. (Two symmetrically located gages were used and the axial strain was calculated from the average of the two readings.) The base length was about 92 mm and the smallest division of the dial gage (a product of Starrett Co.) was 0.0001 inch (0.0025 mm) yielding the strain with the resolution of 10^{-5} (as compared with the typical final value of total strain, 2000×10^{-6}).

A certain error was undoubtedly caused by the fact that the gages were attached to the loading platens rather than to the specimen itself. This was done because of the difficulty in attaching the dial gages to the fragile specimen without cracking it. The error due to the deformation of the steel platens was certainly negligible. The error caused by the deformations localized within the zone of contact between the specimen and the steel platen might have had possibly some significance, but precautions to minimize it were taken by carefully preparing perfectly smooth and perpendicular end surfaces of the specimen (by wet grinding). Some specimens, including all of those for torsion, were glued to the platens with a very thin layer of dental carboxylate cement (which bonds well to wet surfaces); this eliminated the possibility of significant deformation in the contact zone, but the axial strains were consistent with those obtained on unglued platens.

Another error due to attaching the dial gages to the platens stemmed from the fact that friction on the platens inhibits free transverse (radial) deformations of the tube. However, due to the very small wall thickness of the shell, the restraint on the radial deformation was limited to a rather short end zone of the tubular shell. In addition, this restraint did not cause a triaxial confining stress (as in solid specimens) but only a biaxial stress in the wall, and so the effect of the restraint must have been less than that in solid specimens, and probably insignificant.

The possibility of gluing electrical resistance strain gages to the specimen surface was ruled out because, in the first place, the free exchange of moisture with the environment would be prevented by the gage. Strain gages glued on flexible aluminium C-shaped frames spanning between the platens were tried but, in spite of a much higher resolution, were discarded because of difficulties in attaining long-term stability of the gages.

Every loaded test specimen was accompanied by an unloaded companion specimen which was constantly located next to the loaded specimen and was subjected to the same environmental history. At constant temperature, the deformation measured on the companion specimen represented shrinkage. (Actually, the companion specimen received from the dial gage spindle a negligible load of about 0.001 of the axial load of creep specimen.) Creep plus instantaneous strain was determined by subtracting the deformation of the loaded specimen and the companion specimen. Strain of each companion compression specimen was measured by one dial gage which was mounted in the extension of specimen axis on the frame shown in figure 1 and was touching a small steel end plate resting on the specimen.

The loading device for combined axial and torsional loading was considerably more complicated (*Fig.* 1). The torque was developed by a pair of horizontal helical tension springs 180° apart providing a force couple. These springs acted tangentially on the lower platen and were tensioned by a calibrated graduated worm drive mounted on the fixed test frame columns. The lower platen was rotating about specimen axis but fixed against axial movement, being mounted on a preloaded 35° angular contact ball bearing with low breakaway torque. On the other hand, the upper platen was fixed against rotation but free to move axially. It was mounted on a cylindrical stainless steel plunger moving axially in a stainless steel bushing, the two parts having been lapped to fit with a clearance of less than 0.005 mm, thereby achieving excellent lateral stability without axial restraint. The assembly of bushing and plunger was sealed by a bellows and a ring to prevent intrusion of the test atmosphere which would degrade the performance of the device. Both bearings were of very low friction. The axial load was applied on the platens in the same manner as described before (either by three tensile springs tensioned by wing nuts or by the testing machine). The axial movements were measured by two symmetrically placed dial gages, again in the same manner. The rotation of the bottom platen was determined from horizontal circumferential displacements of the platen which were measured by a pair of symmetrically placed dial gages (*Figs.* 1 and 2).

To avoid moisture clogging and corrosion of the dial gage mechanism in the variable test environment, the plastic cover of dial gages was replaced with a watch glass and the whole dial gage was hermetically sealed with « Sluro » plastic rubber. Small brass tubes were fitted to the gage and connected by a small diameter plastic tubing to a small exterior air pump. Room atmosphere was continuously circulated through the interior of the dial gage under slight overpressure.

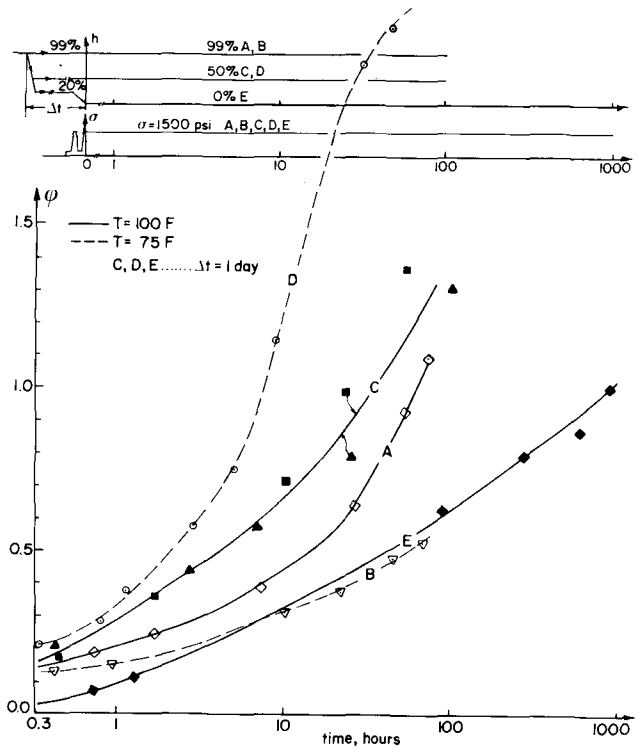

Fig. 4. — Effect of short predrying on axial creep ($10^6\,\varepsilon_{02}$ **for** A...675, B...645, C...773, D...610, E...550).

In case of cyclic loading of many repetitions it was necessary to avoid wear of the dial gage gears by disconnecting the gage during load cycling. This was effected by fitting on the dial gage spindle an extension cylinder containing a teflon piston attached to the spindle. The cylinder was connected by small diameter plastic tubing to an exterior air pump. Except when reading was taken, vacuum was applied during cyclic loading so as to retract the spindle away from the contact. Repeated actuations showed less than 0.0025 mm deviations in readings.

The axial load, P, was always applied by the MTS System following sequence. First a load of magnitude $P/5$ was applied and a strain reading, ε_1, was taken. Then the load was increased (within the time of about 1 min.) to the full value, P, and a reading, ε_2, was again taken. Subsequently the specimen was unloaded to $P/5$, and reading ε_3 was taken. Finally, the load was again increased to the full value, P, reading ε_0 was taken (about 2 min. after ε_1) and the creep test under sustained load started (see *Fig.* 3, e. g.). The purpose of this loading procedure was to minimize the scatter of results. Namely, the statistical scatter of the secant Young modulus, E_{01}, for the first loading (as determined from ε_1 and ε_2) was higher than that for the second loading, E_{02} (as determined from ε_3 and ε_0), which is apparently due to closing of voids and deformations in the end contact of specimen. The average ratio E_{02}/E_{01} was 4/3. The creep strain was defined as $\varepsilon_c = \varepsilon - \varepsilon_0$, where ε = total strain due to load = the strain of the loaded specimen minus the strain of the companion specimen; creep coefficient was defined as $\varphi = \varepsilon_c/\varepsilon_{02}$, with $\varepsilon_{02} = \sigma/E_{02}$.

The torque, however, was always applied in a single, one-way loading procedure because the springs could not be manually tensioned too rapidly. The application of full torque took always about 10 min. and the shear strain γ_0 read right after attaining the full torque was used as the basis of calculating the creep coefficient for shear.

In the spring device for axial loading the springs were also tensioned manually, in a single one-way procedure which took about 10 min. The creep coefficient was in this case calculated as $\varphi = \varepsilon$/strain right after load application. This value of φ is not exactly comparable with that based on second loading. (It is always lower.) However, for lack of data, the φ-values obtained in this manner have been plotted in the figures (curves E in *Fig.* 12, e. g.).

The results for axial creep are plotted in terms of the creep coefficient φ (ratio of creep strain to initial strain). This was preferred to plotting strain per unit stress because of smaller statistical scatter. However, creep per unit stress can be obtained as $\varepsilon_c = \varphi\varepsilon_{02}$ where ε_{02}-values are given in figure captions.

Because the loading sequences for axial load and torsion have not been identical and performed simultaneously, comparison of initial short-time axial strain ε_0 and shear strain γ_0 is difficult, unless a sophisticated computer analysis of test results were made. (Therefore, only the relative changes in $(1+\nu)/(1+\nu_0)$ are plotted in figure 20.)

2.3. Environmental control

The tests of specimens loaded by the testing machine (MTS System) have been carried out in a well insulated, double hinged-door environmental chamber (of interior dimensions $610 \times 381 \times 451$ mm) fitting within the loading frame (*Fig.* 2). The loading columns protruded through air-tightly sealed openings that were cut in the floor and ceiling of the chamber. Dial readings were taken through a front window in the

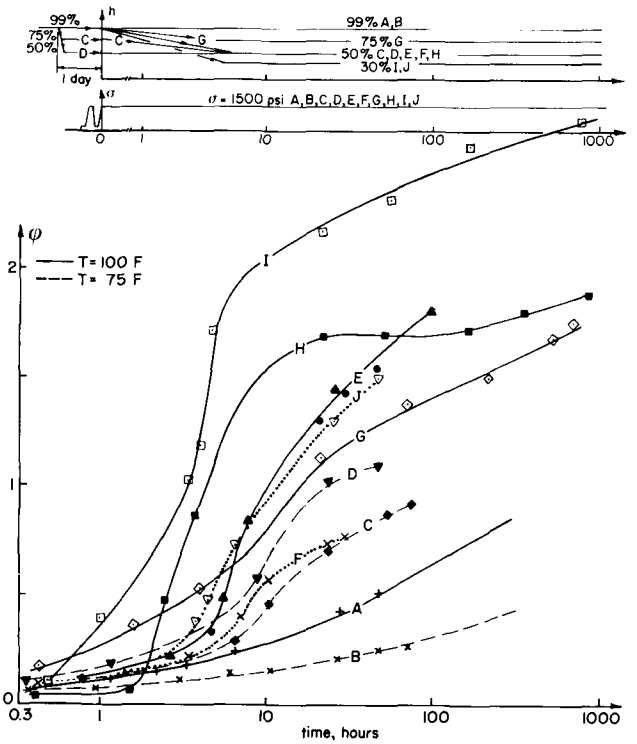

Fig. 5. — Axial creep during drying (curves A and B are averages of 3 specimens each; $10^6\,\varepsilon_{02}$ **for** A...675, B...645, C...550, D...610, E...675, F...592, G...618, H...650, I...633, J...600).

door and hand manipulations inside were possible through sealed openings for hands. The air in the chamber was conditioned to proper relative humidity and temperature by "Aminco-Aire" air-conditioning unit (a product of American Instrument Co. Silver Springs, Maryland) (*Fig.* 2), which had enough power to replace all air in the chamber every minute. The relative humidity of the test atmosphere was controlled by a "Bristol" circular chart programmer-recorder console, the controlled variables being the water bath temperature and the dry bulb temperature, whose time histories were programmed by properly shaped rotating cams. The error in temperature and relative humidity was $\pm$ 0.5°C and $\pm$ 1 %. To assure equal rates of moisture exchange on the external and internal surfaces of the specimens, part of the air coming into the chamber was diverted by an air baffle into a small plastic tubing and was circulated axially through the interior of the specimens, whose platens were equipped with air passages.

The air-conditioning unit was connected to the test chamber by thermally insulated, moisture proof, large-diameter ducts. On the duct of exhaust from the test chamber, a carbon dioxide filter was installed, so as to prevent carbonation of test specimens. The filtering was accomplished by forcing the exhaust air through a barrel in which a saturated water solution of lime ($Ca(OH)_2$) was constantly being sprayed (*Fig.* 2). This altered, of course, the relative humidity of exhaust air, but that did not matter because the relative humidity was readjusted in the air-conditioning unit before return to the test chamber. Because of the slow reactivity of lime with CO_2, the barrel had to be quite large (80 l) and frequently replenished. (If NaOH were used, the filter could have been much smaller but the handing of NaOH would have been much more dangerous).

The specimens loaded by springs and subjected to simple humidity histories were tested in a small, relatively inexpensive, transparent dome-shaped chamber made of Pyrex glass and resting on top of its manually controlled air-conditioning unit which had wet and dry bulb heating elements and was cooled by tap water (a product of Blue M-Electric Company, Chicago) (*Fig.* 2). Here the relative humidity had to be changed in small steps rather than continuously. The air from the chamber was circulated through the interior of the specimens using a small air pump, and external air was circulated through the interior of the dial gages. Several openings were cut through the Pyrex chamber to enable access during the test. Carbon dioxide was removed by "Ascarite" powder (NaOH deposited on inert grains) placed on a tray in the chamber. Specimens to be tested in a perfectly dry atmosphere above room temperature were placed in a well sealed Pyrex glass jar, which in turn was placed in an electric oven controlled by a thermostat (*Fig.* 2). Phosphorus pentoxide (P_2O_5) powder was placed in the jar to absorb all moisture and maintain the relative humidity at 0 %. "Ascarite" powder in the jar was used to absorb carbon dioxide. Both agents were being replenished frequently as they were losing reactivity due to moisture absorption. The Pyrex glass chamber as well as jar were provided with simple devices for remote handling of specimens and tensioning of springs.

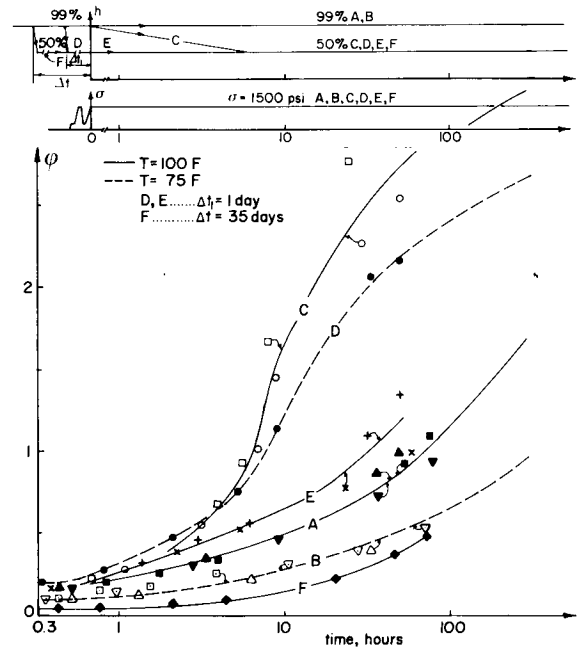

Fig. 6. — Comparison of axial creep of predried and drying specimens (curves A and B are averages of 3 specimens each, C and E of 2 specimens each; $10^6 \varepsilon_{02}$ for A...675, B...645, C...682, D...610×10^{-6}, E...712, F...623).

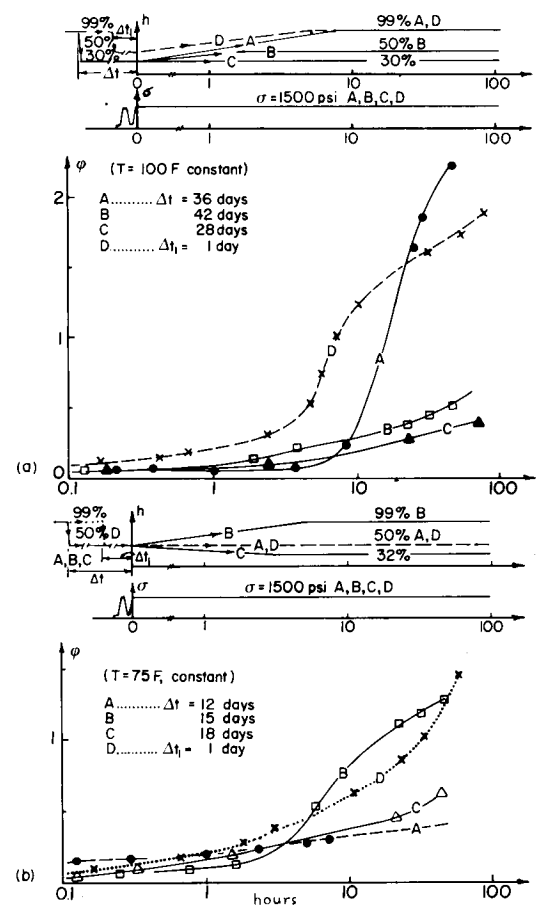

Fig. 7. — Effect of wetting and drying on axial creep of predried specimens : (*a*) $10^6 \varepsilon_{02}$ for A...559, B...669, C...703, D...587; (*b*) A...592, B...621, C...569, D...600.

Additional companion specimens were used in some of the tests to measure moisture loss. These specimens were periodically weighed, suspending them briefly by remote manipulation on a cantilever with a calibrated electric resistance strain gage.

The small thickness of the specimen did not permit the relative humidity h to be changed instantaneously by more than 5 % in the region above 90 % and by more than 10 % in the region 50 to 90 % without causing the specimen to crack longitudinally. Therefore only gradual and continuous change of relative humidity was used, as indicated in the figures. The humidity changes were typically accomplished within 4 to 8 hours. (However, below 50 % an instantaneous change of h is possible without causing a crack.) Specimens have been always carefully examined (with a magnifying glass) for possible cracks and whenever cracks occurred the measurements were excluded. Using the charts from Reference [7], it has been estimated that, for the rate of humidity change used (indicated in figures), the relative humidity within the pores of the specimen probably never deviated by more than about 5 % from the environmental humidity. For such humidity changes, the specimens seldom cracked.

CONCLUSIONS FROM TEST RESULTS

The test results, presented in figures 3-20, do not reveal any surptising new phenomenon which would not be expected on the basis of the thermodynamic theory of creep mechanism ([2], [1], [4]) and would be incompatible with the present experimental knowledge. However, certain properties, which have so far been deduced only from indirect evidence and speculations, are here directly demonstrated apparently for the first time, and are characterized quantitatively. These properties may be summarized as follows:

1. If a specimen which creeps during drying is observed for a sufficiently long time, the slope of the creep curve in the semilogarithmic scale begins to diminish (*Fig.* 5) as the drying process approaches completion. The same is also true for wetting (*Fig.* 7).

2. At lower relative humidities, h, such as 30 to 50 %, the acceleration of creep due to a change in h is smaller and extends for a longer time period than it does at higher humidities, such as 50 to 90 % (*Fig.* 7). However, at very small humidities, such as 0 to 30 %, the acceleration of creep is again more pronounced (*Fig.* 10).

3. Acceleration of creep due to drying is delayed in comparison with weight loss, but the delay does not seem to exceed one month (compare figure 19 and figures 7, 3, and 10).

4. In specimens which have closely approached moisture equilibrium before the creep test, wetting during the creep test accelerates creep similarly as does drying (*Fig.* 7).

5. A change of humidity which begins after the start of the creep test strongly accelerates creep, whether it is negative or positive (*Fig.* 9). At humidities between 50 and 75 % the increase in creep is much larger than it is between 90 and 100 % humidity, but it lags more behind the change of h (*Fig.* 9).

6. Creep recovery strongly depends on humidity and its history. It is lowest at low relative humidity and following the creep which was accelerated by

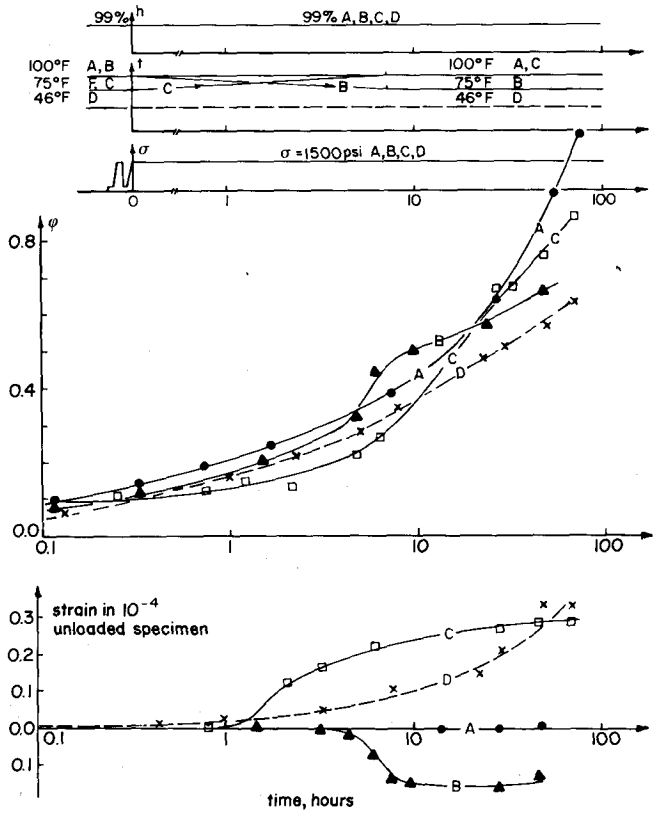

Fig. 8. — Effect of heating or cooling during axial creep ($10^6\ \varepsilon_{02}$ **for** A...675, B...618, C...713, D...600).

simultaneous drying (*Fig.* 12). At 0 % humidity the recovery stops very soon. The highest creep recovery is obtained in saturated specimens (*Fig.* 13).

7. Any change of humidity during creep recovery, whether positive or negative, strongly accelerates and increases the recovery (*Figs.* 12, 13).

8. Effects of humidity changes on the torsional creep and the creep under combined axial force and torque are similar but seem to be somewhat less pronounced (*Fig.* 14).

9. Simultaneous drying, as well as both negative and positive changes of humidity later in the creep test, accelerates the torsional creep (*Fig.* 15). The accelerations in the range 0 to 30 % and near saturation appear to be less, however, than those at intermediate humidities (*Fig.* 15).

10. Torsional creep recovery is higher at higher humidities. The humidity changes after the unloading of torque accelerate the torsional recovery (*Fig.* 18).

11. Change of temperature at constant 75 % humidity during creep accelerates axial creep much more than does the same change at 99 % constant humidity (*Fig.* 8). This is true for temperature rise as well as decrease.

12. Superimposing cyclic load on static load does not appreciably accelerate creep of pure cement paste (*Fig.* 9), which confirms that the cyclic creep of concrete must be due to bond microcracking. The stress-strain diagrams become steeper with a growing number of cycles (as is indicated by the fact thet the increase of strain at the lower limit of stress is higher than it is at the upper limit) (*Fig.* 11).

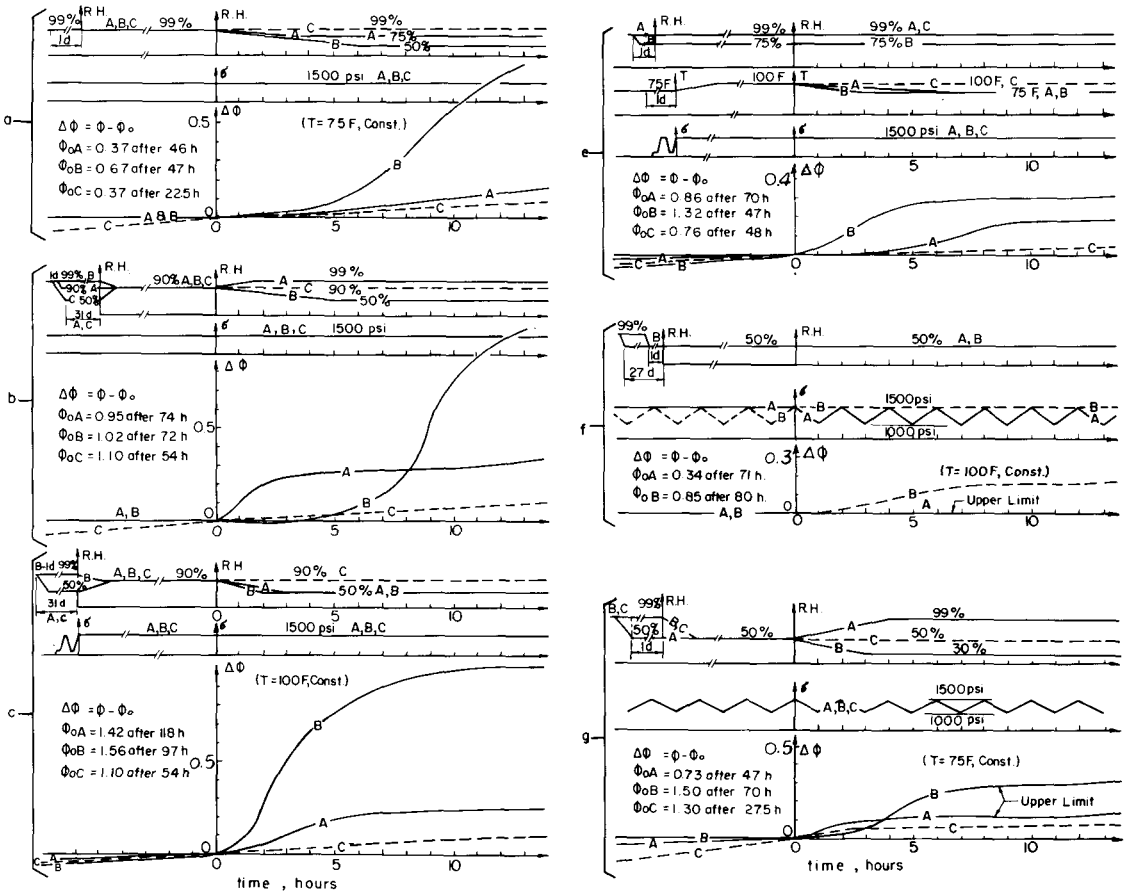

Fig. 9. — Effect of a change in humidity, temperature and load cycling upon axial creep.

13. The effects of humidity changes on creep under cyclic load are essentially the same as they are under static load (*Fig.* 11).

14. Addition of a torque during the axial creep test does not significantly increase the axial creep, and addition of axial load during the torsional creep test does not significantly increase the torsional creep (*Figs.* 16, 17).

15. An increase of humidity which occurs later in the creep test seems to cause reduction of the

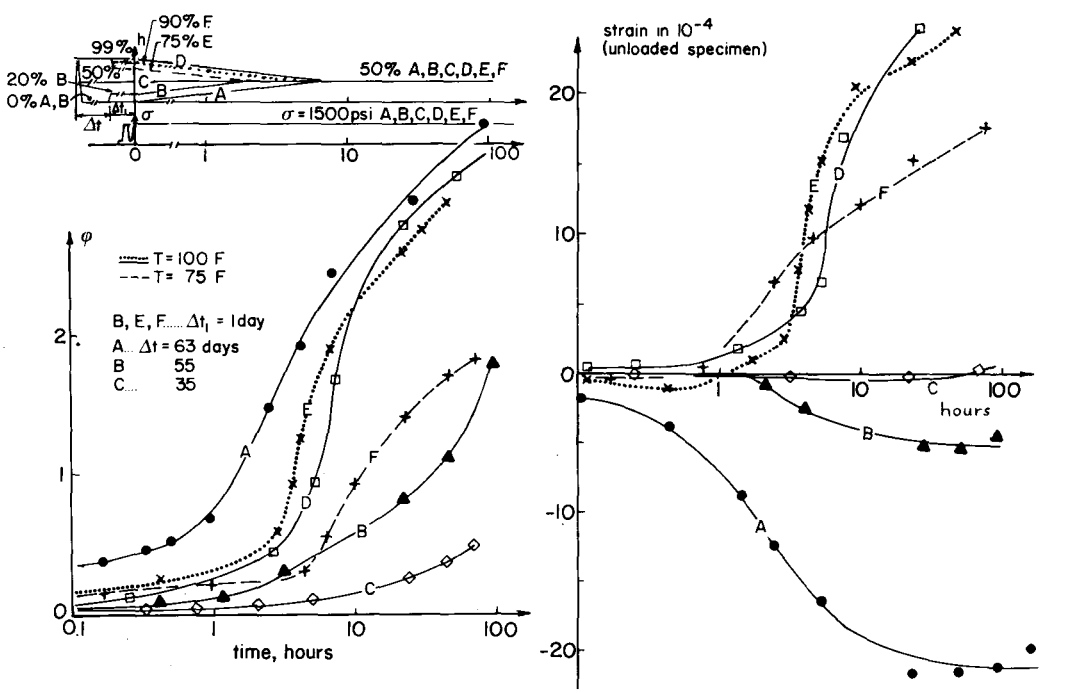

Fig. 10. — Effect of different humidity histories on axial creep ($10^6\,\varepsilon_{02}$ **for** A...562, B...641, C... $\varepsilon_{02}=623$, D... $\varepsilon_{02}=670$, E...637, F...550).

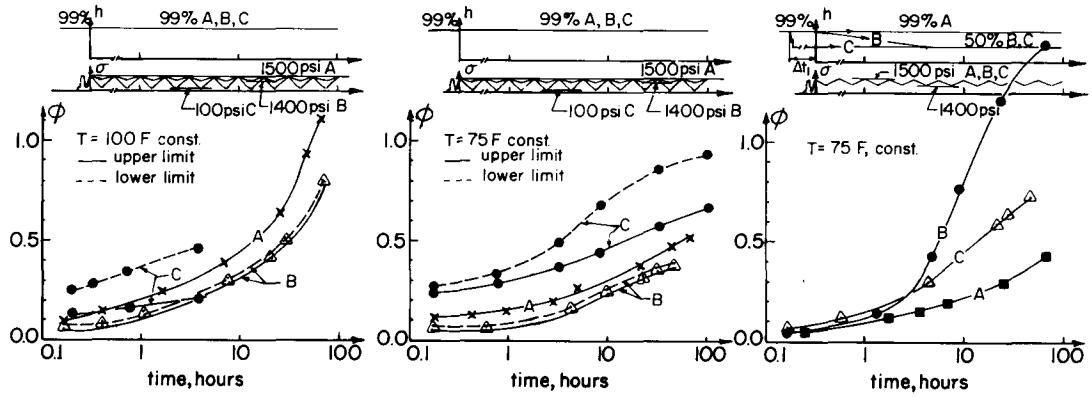

Fig. 11. — Effect of load cycling on axial creep : (*a*) $10^6\,\varepsilon_{02}$ for A...675, B...685, C...500; (*b*) A...645, B...650, C...727; (*c*) A...65, B...619, C...535.

apparent Poisson ratio ν calculated from axial strain ε under stress σ and from shear strain γ under stress τ (i. e., $1+\nu=(\gamma/\tau)/2\,(\varepsilon/\sigma)$); but a decrease of humidity from 100 % seems to increase ν (*Fig.* 20).

16. The time needed to reach the final state of drying, as well as shrinkage, is at least 10-times longer at lower humidities than it is at high humidities (*Fig.* 19) (which agrees with the theory in Reference [5]). A part of shrinkage is delayed with regard to moisture loss, but the delay does not seem to exceed one month (*Fig.* 19).

In addition, several other recently discovered facts are confirmed by the present tests. E. g., in specimens that have had enough time to reach moisture equilibrium, creep is less the lower is the relative humidity (*Fig.* 3).

ACKNOWLEDGMENT

The funding by the U.S. National Science Foundation under Grant Eng 75-14848 No. GK-26030 is gratefully acknowledged.

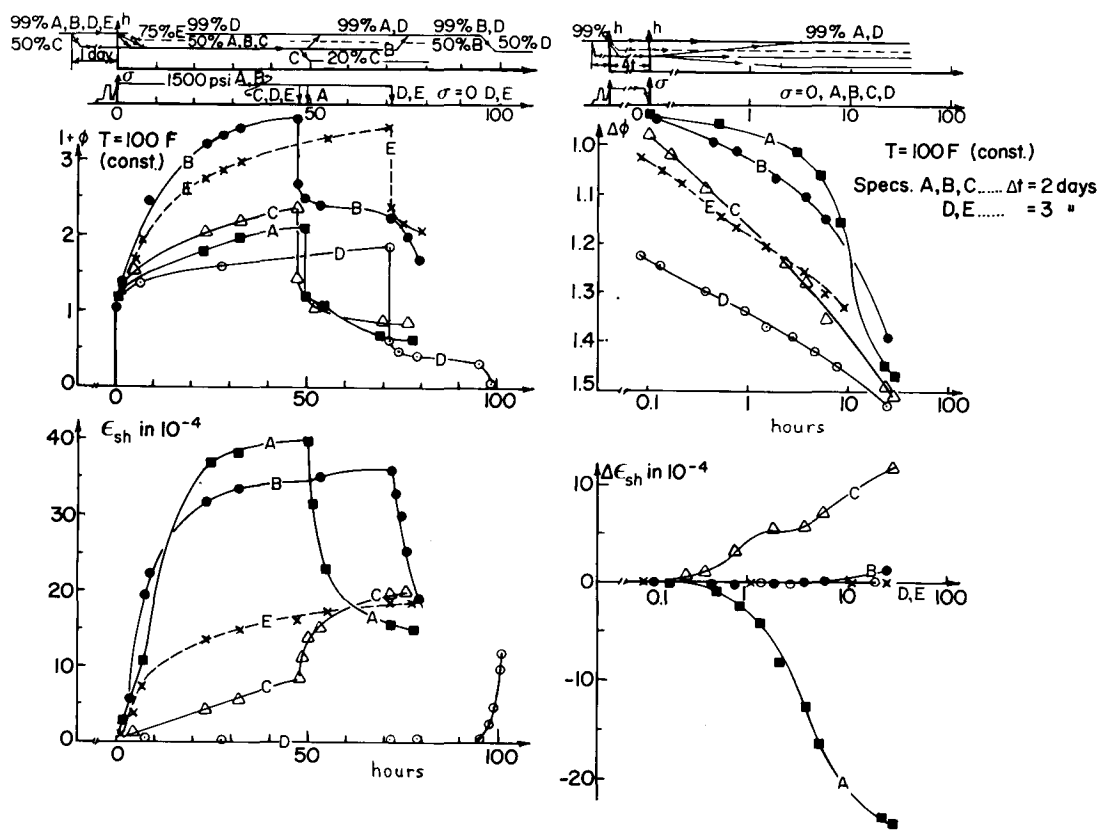

Fig. 12. — Axial creep recovery at varying humidity : (*a*), (*b*) $10^6\,\varepsilon_{02}$ for A...628, B...694, C...651, D...$\Delta\Phi=\Phi-\Phi_0$, $\Phi_0=\Phi$ at $t=0$ (time of unloading), 692, E...647, (*c*), (*d*) t_0 = creep duration before unloading; for A...$\Phi_0=1.10$, $t_0=49$, B...$\Phi_0=2.55$, $t_0=49$ h, C...$\Phi_0=1.36$, $t_0=47$ h, D...$\Phi_0=0.87$, $t_0=71$ h, E...$\Phi_0=2.41$, $t_0=71.5$; $\Delta\varepsilon_{sh}=\varepsilon_0-\varepsilon$, $\varepsilon_0=\varepsilon$ at $t=0$.

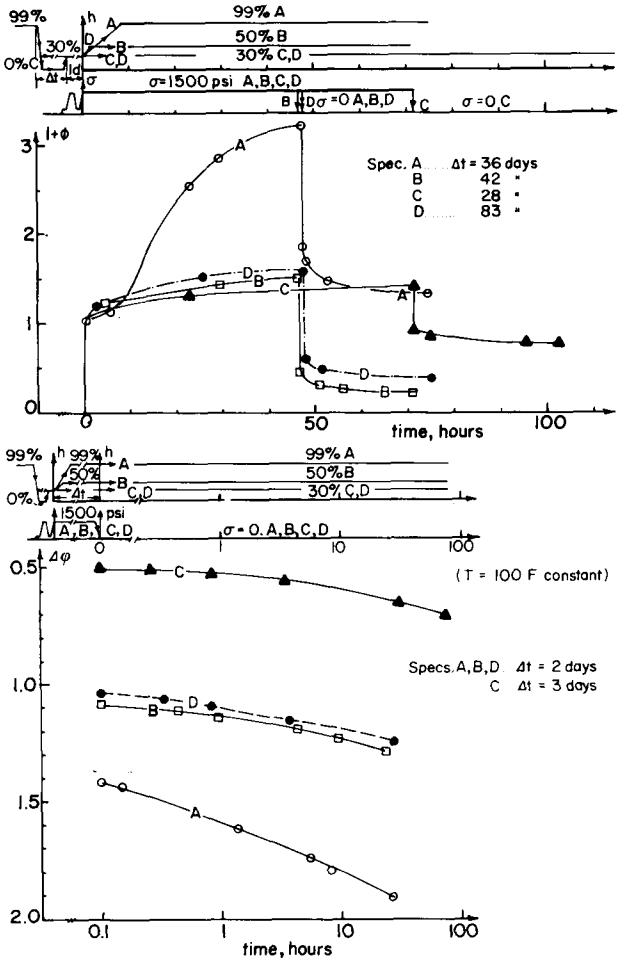

Fig. 13. — Axial creep recovery at various humidities : (*a*) $10^6\ \varepsilon_{02}$ for A...559, B...669, C...703, D...633; (*b*) $\Delta\Phi = \Phi_0 - \Phi$, $\Phi_0 = \Phi$, $t = 0$ (time of unloading), t_0 = creep duration before unloading, A... $\Phi_0 = 2.21$, $t_0 = 47$, *b*... $\Phi_0 = 0.51$, $t_0 = 46.5$ h, C... $\Phi_0 = 0.40$, $t_0 = 71$ h, D... $\Phi_0 = 0.61$, $t_0 = 48$ h.

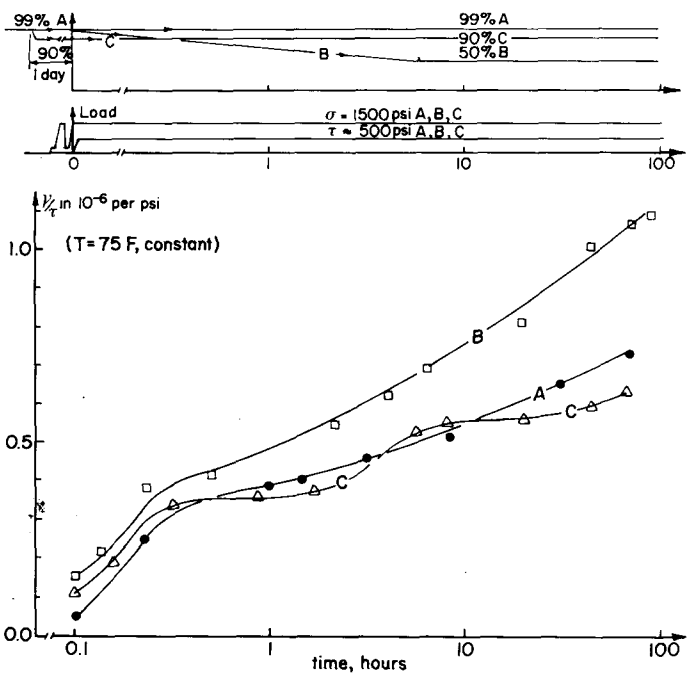

Fig. 14. — Effect of drying on torsional creep (in presence of axial load) $10^6\ \varepsilon_{02}$ for A...380, B...403, C...528, τ for A...500 psi, B...504 psi, C...471 psi.

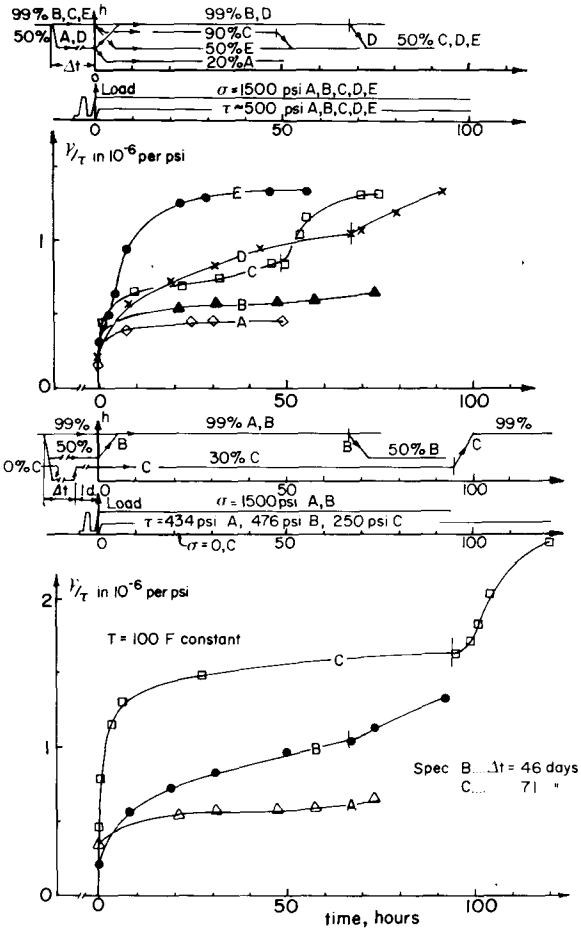

Fig. 15. — Effect of humidity change on torsional creep (in presence of axial load) $10^6\ \varepsilon_{02}$ for A...431, B...530, C...495, D...434, E...485; (*b*) A...530, B...434.

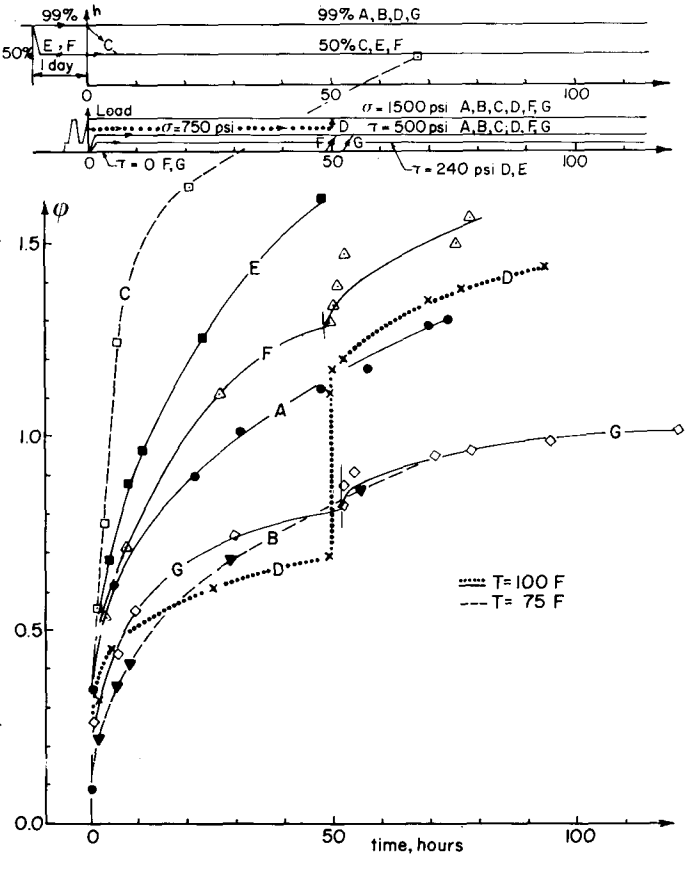

Fig. 16. — Effect of torque change on axial creep ($10^6\ \varepsilon_{02}$ for A = 530, B...300, C...403, D...731, E...416, F...625, G...717; τ for A...434 psi, B...500 psi, C...504 psi, D...244 psi, E...237 psi, F...504 psi, G...498 psi).

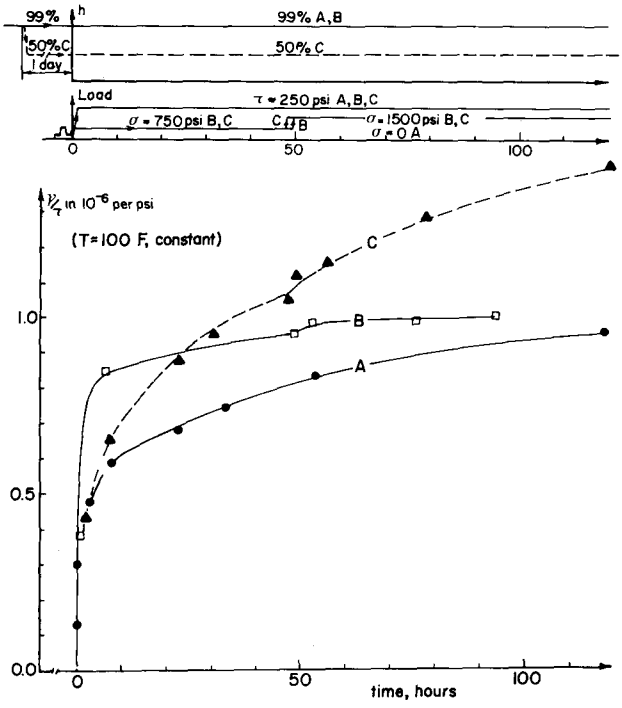

Fig. 17. — Effect of axial load change on torsional creep (with and without drying) (A . . . $\tau = 268$ psi, B . . . $\tau = 244$ psi, $10^6\,\varepsilon_{02} = 731$, C . . . $\tau = 237$ psi, $10^6\,\varepsilon_{02} = 416$).

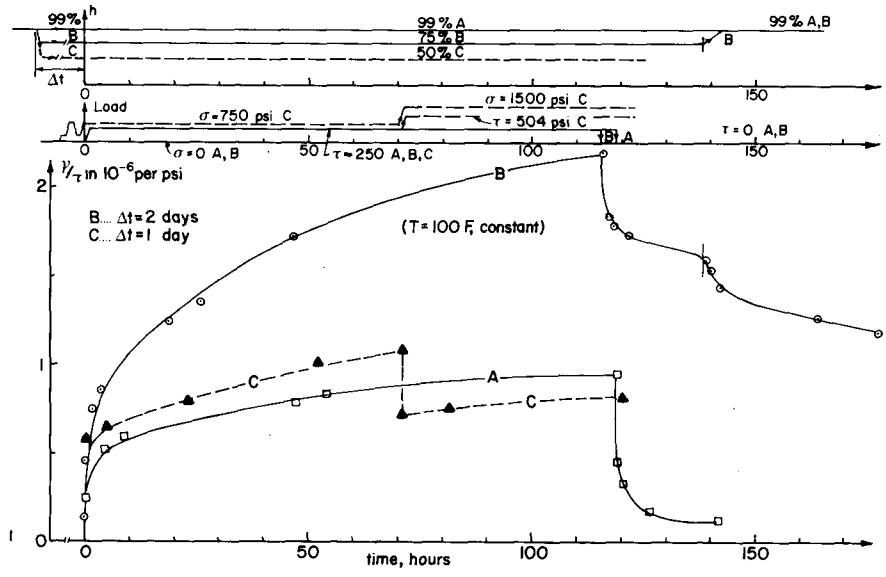

Fig. 18. — Recovery and load step in torsional creep (with and without drying) (A . . . $\tau = 268$ psi, B . . . $\tau = 250$ psi, C . . . $\tau = 252$ psi **(curve C shows a step down because** τ **increases more than** γ**)**.

REFERENCES

[1] BAŽANT Z. P. — *Thermodynamics of interacting continua with surfaces and creep analysis of concrete structures.* Nuclear Engineering and Design, Vol. 20, No. 2, 1972; *see* also Cement and Concrete Research Vol. 2, 1972, pp. 1-16; and Materials and Structures (RILEM), Vol. 3, 1970, pp. 3-36.

[2] BAŽANT Z. P. — *Theory of creep and shrinkage in concrete structures: A précis of recent developments.* Mechanics Today, Vol. 2, 1975, pp. 1-93, ed. by S. NEMAT-NASSER, Pergamon Press.

[3] BAŽANT Z. P., HEMAN J. H., KOLLER H., NAJJAR R. J. — *A thin-wall cement paste cylinder for creep tests at variable humidity and temperature.* Materials and Structures (RILEM), Vol. 6, 1973, pp. 277-328.

[4] BAŽANT Z. P., MOSCHOVIDS Z. — *Surface-diffusion theory for drying creep effect in Portland cement paste and concrete.* Journal of the American Ceramic Society, Vol. 56, No. 5, 1973, p. 235-241.

[5] BAŽANT Z. P., NAJJAR L. J. — *Non linear water diffusion in non saturated concrete.* Materials and Structures (RILEM), Vol. 5, 1972, pp. 3-20; *see* also, Cement and Concrete Research, Vol. 1, pp. 461-473.

[6] L'HERMITE R. — *Volume changes of concrete.* U. S. National Bureau of Standards Monograph 43, 4th Int. Symposium on Chemistry of Cements (held in Washington, D. C.), Vol. 3, 1960, pp. 659-694.

[7] NEVILLE A. M., DILGER W. — *Creep of concrete: Plain reinforced, prestressed.* North-Holland, Amsterdam, 1970.

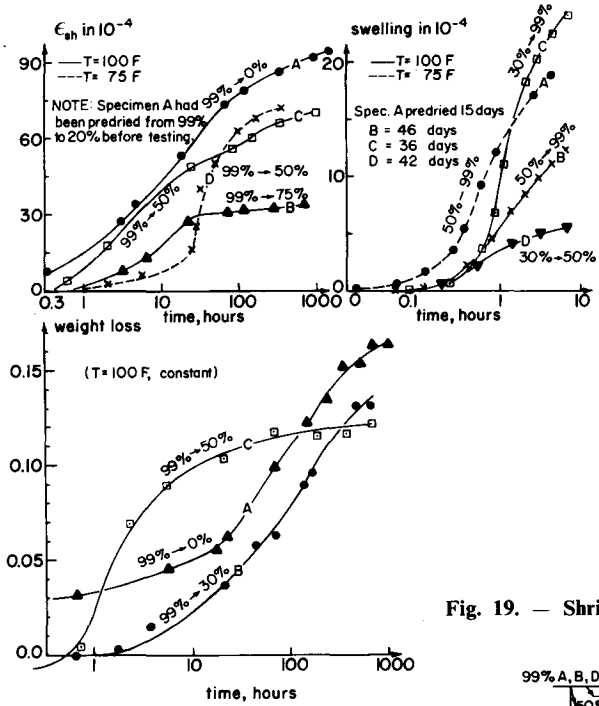

Fig. 19. — Shrinkage, swelling and weight loss.

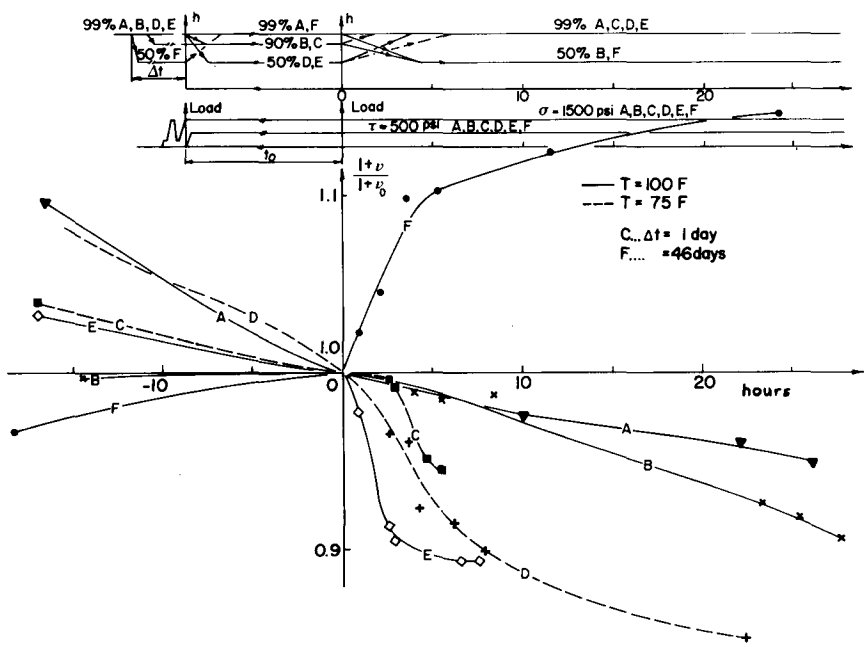

Fig. 20. — Humidity change effect on apparent creep Poisson ratio $v_0 = v$ at $t = t_0$ (time of humidity change).

RÉSUMÉ

Étude expérimentale du fluage de la pâte de ciment Portland durci à différentes teneurs en eau. — *On a réalisé des essais de fluage sous charge axiale et effort de torsion appliqués à des éprouvettes tubulaires à parois extrêmement minces (0,7 mm), ceci dans le but d'assurer des échanges suffisamment rapides d'humidité avec l'ambiance. Les variations d'humidité relative et de température ont été rendues graduelles dans une chambre à ambiance contrôlée à programme, afin de minimiser les différences d'humidité interstitielle dans l'épaisseur de la paroi de l'éprouvette ainsi que les contraintes résiduelles et les micro-fissures qu'on constate en même temps. On a vérifié les conséquences d'états d'humidité et de température antérieurs, y compris celles du séchage avant et durant l'essai de fluage, et celles des variations d'humidité durant l'essai et durant la recouvrance. Les mesures ont révélé une diminution de la pente de la courbe du fluage établie en coordonnées log-t après une période de séchage suffisamment longue; une accélération tant du fluage que de la recouvrance, à la fois par séchage et humidification; une accélération moindre et plus tardive à des humidités plus faibles; un retard de cette accélération par rapport à la perte de poids; une similitude de ces effets en fluage axial et en fluage de torsion; une recouvrance aussi bien qu'un fluage plus prononcé à de plus fortes humidités si l'équilibre en teneur en eau a été approché avant chargement; une plus forte accélération du fluage par augmentation ou diminution de la température pour des humidités au-dessous du point de saturation, mais une plus faible accélération à l'état presque sec; et d'autres effets.*